Published in final edited form as:
Talanta. 2012 January 15; 88: 739–742. doi:10.1016/j.talanta.2011.11.046.

Multiplexed Microneedle-based Biosensor Array for Characterization of Metabolic Acidosis

Philip R. Miller[1], **Shelby A. Skoog**[1], **Thayne L. Edwards**[2], **Deanna M. Lopez**[2], **David R. Wheeler**[2], **Dulce C. Arango**[2], **Xiaoyin Xiao**[2], **Susan M. Brozik**[2], **Joseph Wang**[3], **Ronen Polsky**[2], and **Roger J. Narayan**[1]

[1]Joint Department of Biomedical Engineering, University of North Carolina and North Carolina State University, Raleigh, North Carolina 27695-7115, USA

[2]Department of Biosensors and Nanomaterials, Sandia National Laboratories, Albuquerque, New Mexico 87185, USA

[3]Department of NanoEngineering, University of California at San Diego, La Jolla, California 92093-0448, USA

Abstract

The development of a microneedle-based biosensor array for multiplexed in situ detection of exercise-induced metabolic acidosis, tumor microenvironment, and other variations in tissue chemistry is described. Simultaneous and selective amperometric detection of pH, glucose, and lactate over a range of physiologically-relevant concentrations in complex media is demonstrated. Furthermore, materials modified with a cell-resistant (Lipidure®) coating were shown to inhibit macrophage adhesion; no signs of coating delamination were noted over a 48-hour period.

Keywords

microneedle biosensor; microneedle; multiplexed detection; tumor microenvironment; carbon paste

Pathologic conditions and exercise are associated with alterations in the chemical environment. For example, vigorous exercise can result in metabolic acidosis [1]. In addition to increased fluid pressure and decreased oxygen concentration, alterations in the tissue microenvironment are noted with many tumors [2]. The hypoxic environment of cancer cells along with the Warburg effect (aerobic glycolysis and lactate production by cancer cells) create a microenvironment that is characterized by low glucose concentrations, high lactate concentrations, and low pH levels [3, 4]. Although low pH values are a well-established characteristic of tumor microenvironments [4, 5], the basis of extracellular acidosis is not completely understood. Lactate production is considered to be a main contributor; however,

Corresponding authors: Dr. Roger J Narayan UNC/NCSU Joint Department of Biomedical Engineering Box 7115, Raleigh, NC 27695-7115 Fax: 509-696-8481 roger_narayan@unc.edu Dr. Ronen Polsky Sandia National Laboratories Department of Biosensors and Nanomaterials PO Box 5800, MS-0892 Albuquerque, NM 87185 Fax: 505-845-8161 rpolsky@sandia.gov Dr. Joseph Wang Department of Nanoengineering University California, San Diego La Jolla, CA 92093-0448 Fax: 858-534-9553 josephwang@ucsd.edu.

CO_2 production [6], bicarbonate depletion, ATP hydrolysis, and glutaminolysis may also be contributing factors [7, 8, 9]. In addition, the dynamic nature of cancer cells leads to alterations in metabolism such that cancer cells may rapidly cycle between lactate-producing and lactate-consuming states [10]. While this complex relationship between neoplastic cell proliferation, metabolism, and tumor microenvironment is not entirely understood, this association is observed at the earliest stages of tumor progression [11]. Several areas of study, including genomics, proteomics and metabolomics, can provide insight into signaling pathways and metabolic control of proliferating cancer cells. Furthermore, sensors that enable real time simultaneous detection of multiple biomarkers within the tumor microenvironment may provide additional insight into metabolic acidosis associated with cancer. Novel bioanalytical tools for simultaneous detection of multiple biomarkers may be useful for addressing issues regarding tumor microenvironment and other medically-relevant conditions.

We report the first demonstration of microneedle arrays that have individually addressable sensing microneedles for simultaneous detection of pH, glucose, and lactate. Microneedles offer a novel approach for minimally invasive detection of physiologically-relevant analytes. Initially developed for painless transdermal delivery of pharmacologic agents and vaccines, recent work has shown that hollow microneedle arrays may be used to house microelectrodes for highly sensitive and selective electrochemical detection of physiologically-relevant analytes [12-18]. For example, previous studies have involved the use of hollow microneedle-based devices for electrochemical detection of individual analytes such as ascorbic acid, hydrogen peroxide, lactate, and glucose [12-14]. Owing to the arrayed nature of these microneedle structures, specific target analytes can be detected by each constituent of the array and multiplexed sensing operations can be realized. The multiplexed addressable microneedle array technology that is reported in the present work could lead to a new generation of diagnostic tools for simultaneous detection of a variety of physiologically-relevant analytes.

In this study, microneedle sensors were comprised of a hollow microneedle array that was aligned with strategically placed wells on a commercially-obtained flexible flat cable. Each well had been filled with carbon paste material that was tailored to detect pH, glucose, or lactate (see supplemental information for details). Microneedle arrays were fabricated with a dynamic light micro-stereolithography system using an approach that has been previously described; the microarray design was defined using commercially-obtained computer-aided design software (Figure 1 A) [12]. CO_2 laser ablation was used to create openings in the top insulation layer of the flexible flat cable, exposing the underlying conductors. A layer of single-sided polyester tape was also laser ablated with well patterns that corresponded to the flexible flat cable openings; this structure was aligned and adhered to the flexible flat cable. These wells were subsequently filled with carbon paste (Figure 1 B). This method allowed for each electrode to be addressed by one conductor of the flexible flat cable, which readily interfaced with a circuit board through a low-insertion force connector. A second layer of laser-ablated, double-sided, adhesive-coated tape was used to attach the microneedle array to the flexible flat cable; this structure also served as a fluidic microchannel for the sample. Use of rhodium-modified carbon pastes for detection of glucose and lactate has previously been described [13, 14, 19]. Microneedle paste electrodes for detection of pH were created by chemically depositing Fast Blue RR diazonium salt; the electrodes were subsequently washed with deionized water [20]. Calibration of chemically modified carbon pastes for detecting alterations in pH was performed in 0.1 M phosphate buffer over a 5.0-8.0 pH range at intervals of 0.5 pH units. Cyclic voltammetric scans were performed from -0.7 V to 0.8 V at 100 mV/s against external Ag/AgCl reference and Pt counter electrodes. The pH response was measured by evaluating the shift of the anodic peak potential position of the quinone moiety on the immobilized Fast Blue RR salt. Figure 2 shows the calibration curve

for chemically modified carbon paste strips. Increasing buffer acidity caused a negative shift in the anodic peak potential; a highly linear relationship over the entire tested pH region (R^2=99%) demonstrated that the sensors within the integrated carbon paste microneedle platform were capable of pH monitoring.

The responses for individual wells tailored for glucose and lactate detection were assessed in 0.1 M phosphate buffer. Testing for pH values of 5, 6, 7, and 7.5 against an outside Ag/AgCl reference and Pt counter electrode was performed. This pH range included normal physiological levels for interstitial fluid [11]; pathologic (increased acidity) levels were also evaluated. The chronoamperometric detection potentials for glucose and lactate sensing were selected because they were previously shown to catalytically reduce enzymatically-produced peroxide while minimizing responses of common interfering electroactive species such as ascorbic acid, uric acid, and acetaminophen [19]. For glucose, a fixed detection potential of -0.05 V was used. Figure 3 shows calibration curves generated from chronoamperometric scans for each of the pH regions. The responses were linear from 2 mM to 12 mM for each buffer pH; the magnitude of the current response could readily be distinguished, indicating fingerprint detection of glucose is possible for specific pH values. Lactate analysis was performed using a detection potential of -0.15 V. Linear responses were noted over physiologically-relevant concentration values; responses characteristic of each of the pH values were observed (Figure 4).

Multiplexed real time detection mandates investigation into whether simultaneous analysis of several markers can be performed with a high degree of accuracy and with minimal cross-talk. We performed analysis of mixtures containing glucose and lactate at a fixed pH value with the integrated carbon paste microneedle platforms. Figure 5 shows the response from the lactate microneedle portion of the array before and after addition of glucose (as indicated by green and red curves, respectively). The addition of 4 mM glucose had no effect on the response of the lactate oxidase-modified paste. Subsequent addition of 4 mM lactate produced a current response of ~38 nA, which is consistent with the expected value for a solution with a pH of 7 (based on Figure 4). The pH value was simultaneously confirmed from the on-array response of the Fast Blue RR-modified microneedle (inset).

In this same solution, the glucose oxidase-modified microneedle was tested from its fixed potential chronoamperometric response (Figure 6). After stabilizing to a steady state current, the addition of 4 mM lactate resulted in no response on the electrode. Subsequently, a 4 mM addition of glucose created an increase in reduction current (~10 nA), which corresponded to the expected value for the glucose concentration based on Figure 3. This data confirmed that each of the electrodes in the array is capable of performing analyte-specific detection in a complex environment.

In previous work, the E-shell 300 acrylate-based polymer used for microneedle fabrication showed suitable cytotoxicity against both human epidermal keratinocytes and human dermal fibroblasts [21]. Many implantable continuous monitoring systems succumb to biofouling, which is associated with protein, macrophage, and fibroblast adhesion as well as tissue encapsulation at the implantation site [22]. We investigated whether a passive coating could limit adhesion of macrophages to the acrylate-based polymer used for microneedle fabrication. Lipidure®, a copolymer of butyl methacrylate and 2-methacryloyloxyethyl phosphorylcholine, was chosen as the coating material; this material has been previously shown to reduce the adherence of fibroblasts on poly(ethylene telephthalate) in comparison with uncoated material [23]. In previous work, Mang et al. and Ayaki et al. [24, 25] showed using in vitro studies that Lipidure® materials provide good cytocompatibility. To determine the effectiveness of Lipidure®-coated E-shell 300 materials in preventing macrophage adhesion, we examined uncoated materials and coated materials (n=3) at 2 hours, 24 hours,

and 48 hours (data not shown) after seeding. Following each time point, the materials were imaged in growth medium with a fluorescent microscope. Figure 7 shows macrophage-material interaction at 2 and 24 hours post seeding for both coated and uncoated materials. Uniform macrophage coverage was noted on the uncoated materials; on the other hand, the coated materials displayed little to no cell attachment. The few cells located on the coated materials demonstrated bunched morphologies, indicating poor adhesion. This trend continued through the subsequent time points; the uncoated material maintained a similar number of adherent cells while the coated material contained little to no adherent cells. All of the images showed that the coating did not delaminate from the E-shell 300 substrate for each tested time point; adhesion is a critical factor that determines coating functionality. These results indicate that the Lipidure® coating showed adhesion to E-shell 300 and resistance to macrophage adhesion over the tested time period. Future studies need to be performed to evaluate the relationship between coating thickness and cell attachment as well as the relationship between skin insertion force and coating adhesion.

In conclusion, we have developed a microneedle-based sensor array that is capable of simultaneously detecting multiple analytes in physiologically-relevant tissue environments. The modified microneedles selectively detected changes in pH, lactate, and glucose, indicating potential use for characterizing complex biological environments such as those seen in vigorous exercise and tumor microenvironments. The devices showed suitable performance when tested over physiologically-relevant concentration ranges for each analyte; in addition, the devices showed no signs of adverse responses in complex solutions. Furthermore, the acrylate-based polymer used for microneedle fabrication was coated with a material that limited macrophage adhesion over a 48-hour period. We envision that this sensor technology could be useful to both biomedical research and clinical medicine communities [26].

Supplementary Material

Refer to Web version on PubMed Central for supplementary material.

Acknowledgments

Sandia is a multiprogram laboratory operated by Sandia Corporation, a Lockheed Martin Company, for the United States Department of Energy's National Nuclear Security Administration under Contract DE-AC04-94AL85000. The authors acknowledge the Sandia National Laboratories' Laboratory Directed Research & Development (LDRD) program. We would like to acknowledge Bryan Carson for providing the RAWRGTAPCP cell line with Mcherry and GFP reporters.

References

1. Robergs RA, Ghiasvand F, Parker D. Am. J. Phys. 2004; 287:R502.
2. Rofstad EK. Int. J. Radiat. Biol. 2000; 76:589. [PubMed: 10866281]
3. Vander Heiden MG, Cantley LC, Thompson CB. Science. 2009; 324:1029. [PubMed: 19460998]
4. Warburg O, Wind F, Negelein EJ. Gen. Physiol. 1927; 8:519.
5. Evelhoch, JL. The Tumour Microenvironment: Causes and Consequences of Hypoxia and Acidity (Novartis Foundation Symposium 240). Goode, JA.; Chadwick, DJ., editors. John Wiley & Sons; Chichester, UK: 2008. p. 68-84.
6. Helmlinger G, Sckell A, Dellian M, Forbes NS, Jain RK. Clin. J. Cancer Res. 2002; 8:12841.
7. Vaupel P, Kallinowski F, Okunieff P. Cancer Res. 1989; 49:6449. [PubMed: 2684393]
8. Tannock IF, Rotin D. Cancer Res. 1989; 49:4373. [PubMed: 2545340]
9. Medina MA, Sánchez-Jiménez F, Márquez J, Rodríguez Quesada A, Núñez I. Mol. Cell. Biochem. 1992; 113:1. [PubMed: 1640933]
10. Semenza GL. J. Clin Invest. 2008; 118:3835. [PubMed: 19033652]

11. Cardone RA, Casavola V, Reshkin SJ. Nature Rev. Cancer. 2005; 5:786. [PubMed: 16175178]
12. Miller PR, Gittard SD, Edwards TL, Lopez DM, Xiao X, Wheeler DR, Monteiro-Riviere NA, Brozik SM, Polsky R, Narayan RJ. Biomicrofluidics. 2011; 5:013415.
13. Windmiller JR, Zhou N, Chuang MC, Valdés-Ramírez G, Santhosh P, Miller PR, Narayan R, Wang J. Analyst. 2011; 136:1846. [PubMed: 21412519]
14. Windmiller JR, Valdés-Ramírez G, Zhou N, Zhou M, Miller PR, Jin C, Brozik SM, Polsky R, Katz E, Narayan R, Wang J. Electroanal. 2011; 23:2302.
15. Ricci F, Moscone D, Palleschi G. IEEE Sensors J. 2008; 8:63.
16. Zimmermann S, Fienbork D, Flounders AW, Liepmann D. Sens. Actuat. B. 2004; 99:163.
17. Henry S, McAllister DV, Allen MG, Prausnitz MR. J. Pharm. Sci. 1998; 87:922. [PubMed: 9687334]
18. Prausnitz MR. Adv. Drug Deliv. Rev. 2004; 56:581. [PubMed: 15019747]
19. Wang J, Chen L, Liu J. Electroanalysis. 1997; 9:298.
20. Makos MA, Omiatek DM, Ewing AG, Heien ML. Langmuir. 2010; 26:10386. [PubMed: 20380393]
21. Gittard SD, Miller PR, Boehm RD, Ovsianikov A, Chichkov BN, Heiser J, Gordon J, Monteiro-Riviere NA, Narayan RJ. Faraday Discuss. 2011; 149:171. [PubMed: 21413181]
22. Anderson JM, Rodriguez A, Chang DT. Semin. Immunol. 2008; 20:86. [PubMed: 18162407]
23. Ishihara K, Ishikawa E, Iwasaki Y, Nakabayashi N. J. Biomater Sci. Polym. Ed. 1999; 10:1047. [PubMed: 10591131]
24. Ayaki M, Iwasawa A, Niwano Y. Jpn. J. Opthalmol. 2011; 55:541.
25. Mang A, Pill J, Gretz N, Kraenzlin B, Buck H, Schoemaker M, Petrich W. Diabetes Technol. Ther. 2005; 7:163. [PubMed: 15738714]
26. Brizel DM, Scully SP, Harrelson JM, Layfield LJ, Bean JM, Prosnitz LR, Dewhirst MW. Cancer Res. 1996; 56:941. [PubMed: 8640781]

Highlights

- Microneedle-based array capable of simultaneous detection of multiple analytes
- Changes in pH, lactate, and glucose detected
- Performance demonstrated for physiologically-relevant concentration ranges

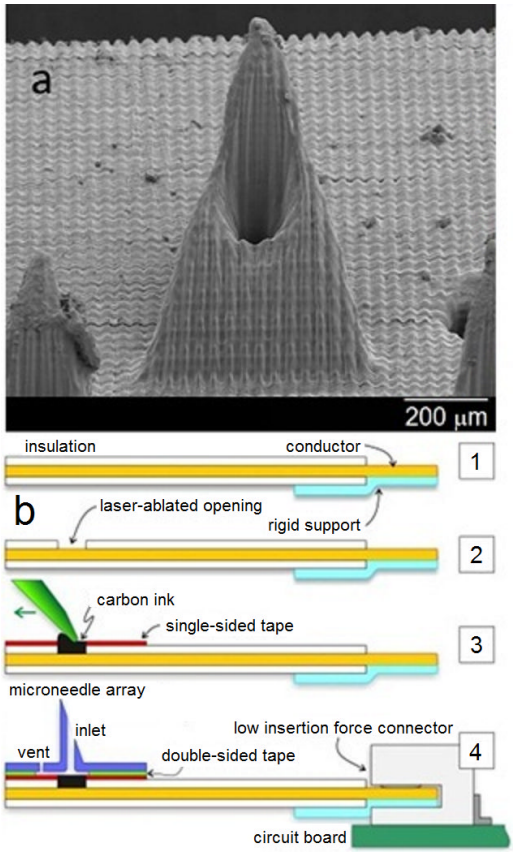

Figure 1.
Scanning electron micrograph of a single microneedle (A) and schematic of the microneedle-biosensor assembly (B).

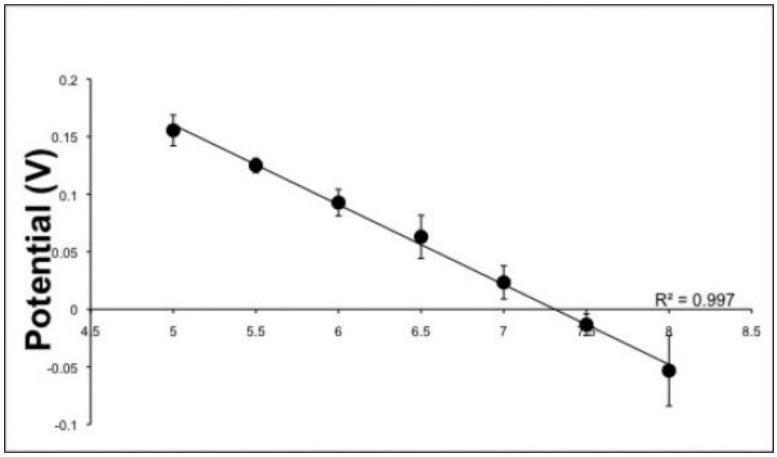

Figure 2.
Calibration curves of a chemically modified carbon paste electrode in 0.1 M phosphate buffer (pH 5.0-8.0 at 0.5 intervals) against an outside Ag/AgCl and Pt reference and counter electrode, respectively.

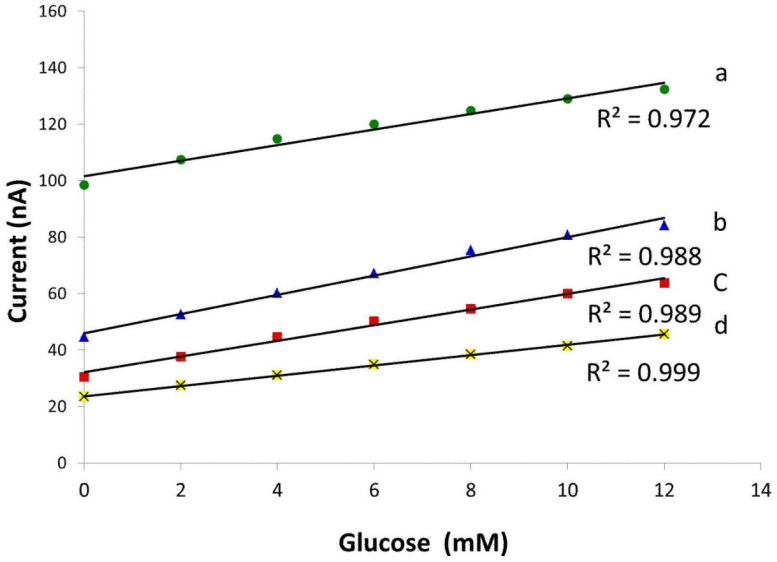

Figure 3.

Calibration curves of carbon paste containing glucose oxidase in 0.1 M phosphate buffer (pH 5.0, 6.0, 7.0 and 7.5 are indicated by a, b, c, and d, respectively) against an outside Ag/AgCl and Pt reference and counter electrodes with a detection potential of -0.05 V. Data were obtained from the current response after 5 seconds.

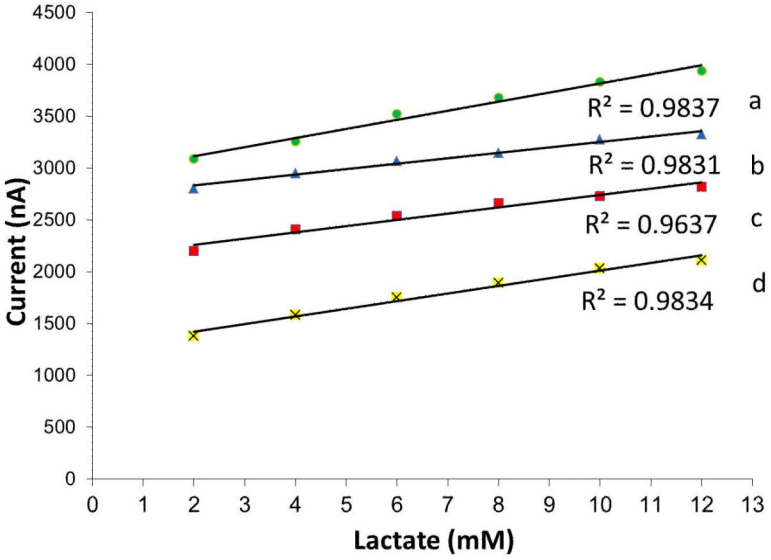

Figure 4.

Calibration curves of carbon paste-containing lactate oxidase in 0.1 M phosphate buffer (pH 5.0, 6.0, 7.0 and 7.5 are indicated by a, b, c, and d, respectively) against an outside Ag/AgCl and Pt reference and counter electrode with a detection potential of -0.15 V.

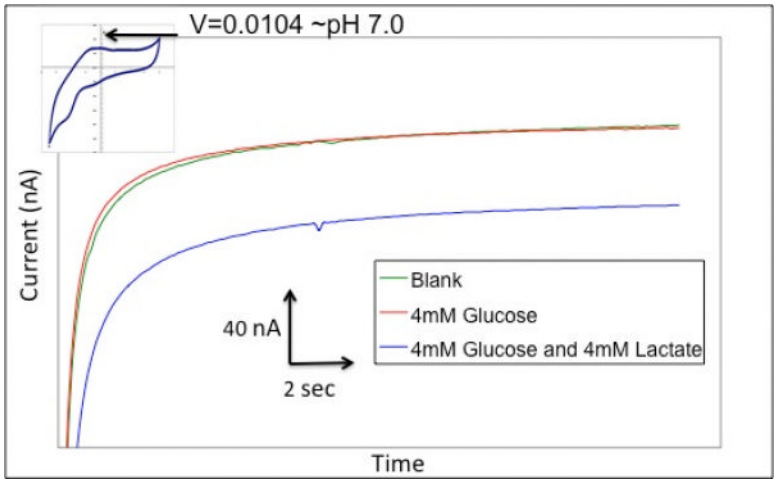

Figure 5.
Selectivity of the lactate electrode. Figure shows three scans in the order of a blank solution, 4 mM glucose, and 4 mM lactate. Inset: Cyclic voltammogram of Fast Blue-modified carbon paste microneedle.

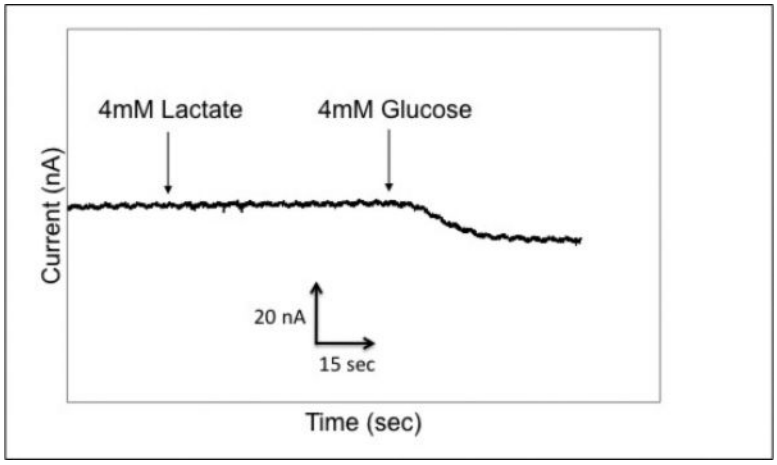

Figure 6.
Selectivity of the glucose electrode.

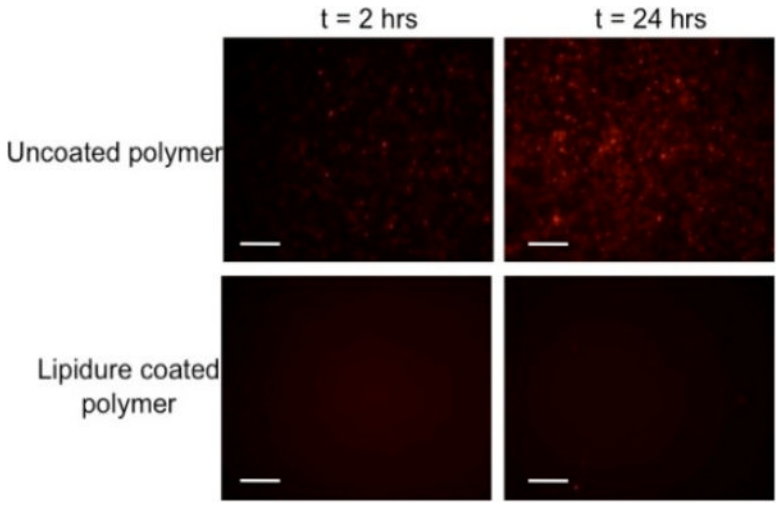

Figure 7.
Fluorescent images of macrophage adhesion to uncoated and Lipidure®-coated E-shell 300 acrylate-based polymer at 2 and 24 hours post seeding (200 μm scale bar).